Optics Communications 536 (2023) 129299

Contents lists available at ScienceDirect

Optics Communications

journal homepage: www.elsevier.com/locate/optcom

Tunable optoelectronic oscillator based on a high-Q microring resonator

Tian Cui [a], Dapeng Liu [b], Fengyuan Liu [a], Zhijian Zhang [a], Zhenzhou Tang [a,*], Naidi Cui [b], Shilong Pan [a,*]

[a] Key Laboratory of Radar Imaging and Microwave Photonics, Ministry of Education, Nanjing University of Aeronautics and Astronautics, Nanjing 211106, China
[b] United Microelectronics Center, Chongqing 401332, China

ARTICLE INFO

Keywords:
Optoelectronics oscillator
Microring resonator
Microwave photonic filter
Phase noise

ABSTRACT

This paper proposes a tunable optoelectronic oscillator (OEO) by using a silicon nitride high-Q microring resonator (MRR) with a Q value of 4.36×10^5. Inserting the high-Q MRR into a phase-modulated link, an 8–38 GHz tunable microwave photonic filter (MPF) is realized with a 3-dB bandwidth of ~610 MHz. Based on the tunable MPF, a tunable OEO is established. The frequency range of the OEO is 14.60 to 25.65 GHz, and the measured phase noise of the 25.65-GHz oscillation signal is -88 dBc/Hz@10 kHz.

1. Introduction

Optoelectronic oscillator (OEO) is an ideal signal source that can generate microwave signals with high spectral purity (the side-mode suppression ratio can reach > 60 dB) and low phase noise (currently, the lowest can reach −163 dBc/Hz@10 kHz [1]). However, most of the conventional OEOs are built by discrete devices, which makes it difficult to be applied to the platforms such as UAVs and satellites due to their large size and high cost. Therefore, an integrated OEO is highly desirable.

As early as 2008, a voltage-controlled whispering gallery mode (WGM) resonator is used to replace the bulky fiber loop in the conventional OEO. By altering the voltages of the WGM, a 34–36 GHz RF signal can be obtained [2]. However, the WGM is hard to fabricate and is almost impossible to be integrated with other electro-optic devices. Another kind of integrated OEO is based on a resonant tunneling diode-photodetector-laser diode (RTD-PD-LD) [3] or an electro-absorption modulated laser (EML) [4]. Although the structure is simplified because light generation, modulation, and photodetection can be implemented by a single device, a long optical fiber loop (several kilometers) is still required. Recently, owing to the improvements in silicon photonics, some silicon-photonics-based solutions have been reported. For instance, a silicon microring resonator (MRR) is functioned as an optical bandpass filter to select the oscillation mode [5,6]. By simply adjusting the wavelength spacing between the MRR and the laser source, the OEO can be tuned within 6–18 GHz. Because of the relatively large loss of the silicon waveguide (typically 1~2 dB/cm), the Q-factor of the MRR is only 8.1×10^4 and the phase noise of the OEO is only ~−50 dBc/Hz@10 kHz. In addition, a race-track MRR is designed to realize a tunable microwave photonic filter (MPF) [7] and then an OEO with a frequency range of 0–20 GHz is obtained based on it [8]. In these works, the widths of the race-tracks should be increased to reduce the loss, the complexities in design and fabrication are both increased.

In [9], by simultaneously integrating a high-speed phase modulator (PM), a thermally adjustable microdisk resonator (MDR), and a high-speed PD on a single silicon-on-insulator (SOI) chip, a miniaturized OEO with a frequency range of 3–8 GHz is achieved. The Q-factor of the MDR is about 1.1×10^5, and the phase noise of the OEO is only −80 dBc/Hz@10 kHz. By the similar tuning principle, a broadband tunable OEO based on a high-Q silicon nitride MDR is also proposed [10]. A low phase noise (−120 dBc/Hz@10 kHz) is achieved by employing the PT symmetric mechanism. However, due to the different modulation efficiencies of different modes in PM, it is difficult to balance the gain and loss of the loop and the side-mode suppression ratio (SMSR) of the system is lower than the current average level. To increase the integration degree, a fully-integrated OEO is firstly realized by monolithically integrating all the required electrical and optical devices on an InP-based chip [11]. Due to the significant loss of the InP waveguide, only an 8.97-mm oscillating loop is fabricated on the chip. As a result, the phase noise is only −60 dBc/Hz@10 kHz, which actually cannot meet the requirements of almost all the systems.

In this paper, a high-Q MRR for mode selection is fabricated on the silicon nitride platform. The full width at half maximum (FWHM) of the MRR is ~3.55 pm and a Q-factor of 4.36×10^5. Then, an 8–38 GHz tunable MPF with a 3-dB bandwidth of ~610 MHz is built by inserting the high-Q MRR into a phase-modulated link. Based on the tunable MPF, a tunable OEO is established. The measured frequency range of the OEO is 14.60 to 25.65 GHz, and the phase noise of the 25.65-GHz oscillation signal is −88 dBc/Hz@10 kHz.

* Corresponding authors.
E-mail addresses: tangzhzh@nuaa.edu.cn (Z. Tang), pans@nuaa.edu.cn (S. Pan).

https://doi.org/10.1016/j.optcom.2023.129299
Received 16 June 2022; Received in revised form 3 January 2023; Accepted 21 January 2023
Available online 2 February 2023
0030-4018/© 2023 Elsevier B.V. All rights reserved.

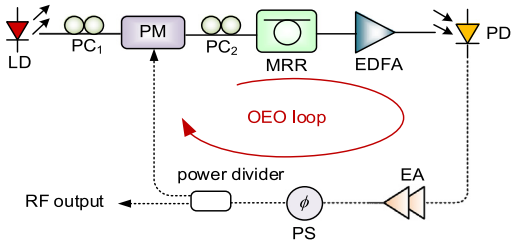

Fig. 1. Schematic diagram of the MRR-based OEO. LD: laser diode, PC: polarization controller, PM: phase modulator, MRR: microring resonator, EDFA: erbium-doped fiber amplifier, PD: photodetector, EA: electrical amplifier, PS: phase shifter, OEO: optoelectronic oscillator.

2. Principle

Configuration of the proposed OEO is illustrated in Fig. 1. An optical carrier generated by an LD is sent to a PM after passing through a polarization controller (PC, PC1). The output of the PM is then coupled into the MRR with its polarization state adjusted to be TE mode by another PC (PC2). When the light goes through the on-chip all-pass MRR, it is coupled out of the chip and applied to a PD after being amplified by an erbium-doped fiber amplifier (EDFA). According to the principle of phase modulation, if one of the sidebands falls into the resonance of the MRR to break the amplitude balance of the phase modulation, the phase-to-amplitude modulation is achieved, and a microwave signal can be obtained after photodetection. Therefore, the entire process can be regarded as a bandpass MPF [12]. Then the microwave signal is divided into two paths after passing through the power divider. One portion is used for RF output and the other is fed back to the RF port of the PM to construct an OEO loop. An electrical amplifier (EA) is employed to provide sufficient gain and a phase shifter (PS) is applied to adjust the phase.

Obviously, the quality of the OEO mainly depends on the performance of the MPF. Since the frequency spacing between the optical carrier and the resonance determines the center frequency of the MPF, the OEO frequency tuning can be easily implemented by simply changing the carrier wavelength or the MRR resonant wavelength. Besides, the MPF bandwidth is proportional to the spectral response of the MRR, so a high-Q MRR is required.

Since the Q-factor of the MRR is mainly dependent on the loss of the waveguide [13], and the silicon nitride integrated platform can greatly reduce waveguide loss under the premise of ensuring proper integration compared with the SOI platform, a low-loss silicon nitride platform (CUMEC, 300 nm silicon nitride process CSiN300) based on the low-pressure chemical vapor deposition (LPCVD) technology is employed to fabricate the high-Q MRR.

Fig. 2(a) presents the microscope image of the high-Q MRR, and the vertical view and left view are shown in Fig. 2(b) and Fig. 2(c). The MRR consists of a circular waveguide with a radius of 165 μm and the gap between the long waveguide and the circular waveguide is 2.3 μm. The thickness of the waveguide is 300 nm and the width is 1 μm. By measuring the insertion losses of a series of waveguides with different lengths ranging from 0 cm to 35 cm, and linear fitting the relationship between the insertion losses and waveguide length, the waveguide loss can be obtained from the slope of the linear fitting curve, which is about 0.1 dB/cm at 1550 nm. At the same wavelength, the group refractive index is about 1.8935, which is calculated by measuring the spectrum of the asymmetric Mach–Zehnder interferometer.

A vertical coupling is used to achieve optical coupling between the fibers and the on-chip MRR. Six adjusters are used to adjust the position and angle of the optical fiber to minimize the coupling loss. In our experiment, the coupling loss is about 13 dB. Fig. 2(d) depicts the spectral response of the MRR. The FWHM of the MRR is measured to be 3.55 pm (~444 MHz), so the Q-factor is calculated to be 4.36×10^5. In addition, the free spectral range (FSR) is 1.21 nm, and the extinction ratio reaches 12.23 dB.

3. Experiment

Fig. 3 shows the experimental setup of the proposed OEO. A tunable optical carrier is generated by a tunable LD (Teraxion PS-NLL) and sent to a PM (EOSPACE) with a bandwidth of 30 GHz. When passing through the on-chip MRR, the optical signal is amplified by an EDFA (KEOPSYS CEFA-C-HG) with a gain of 50 dB and sent to a 50-GHz PD (Finisar XPDV2120R) with a responsivity of 0.65 A/W. Then the output signal is divided into two portions, one of which is applied to the PM to build an OEO loop. The other is sent to a phase noise analyzer (R&S FSWP26) for spectrum and phase noise characterizations. It should be noted that an EA with a gain of 40 dB and a microwave phase shifter (PS) are also inserted in the OEO loop to provide loop gain and to adjust the microwave phase, respectively.

Fig. 4(a) shows the measured frequency response of the MPF, when using an optical carrier with a fixed wavelength of 1550.12 nm. The 3-dB bandwidth of the MPF, at a center frequency of 25.5 GHz, is ~610 MHz, and the stopband rejection ratio that is defined as the amplitude ratio of the passband to the closest stopband reaches 18.3 dB. In this condition, the oscillation frequency of the OEO is ~25.65 GHz, which is shown in Fig. 4(b). The power of the oscillation signal is 6.42 dBm, and the SMSR, i.e., the power ratio of the main mode to the nearest side mode, is about 49.47 dB. It can be seen from Fig. 4(c) the FSR of the tunable OEO is about 5 MHz. Besides, the phase noise is measured to be −88 dBc/Hz@10 kHz, which is presented in Fig. 4(d).

Fig. 5(a) shows the temperature variation of the spectral response of the MRR. As can be seen, when the temperature increases, the resonant wavelength moves to the longer wavelength. The corresponding relationship between the oscillation frequency of the OEO and the temperature of MRR is illustrated in Fig. 5(b). The output wavelength of the LD is fixed at 1550.12 nm. It can be observed that the oscillation frequency of the OEO decreases with the increase of temperature. There is a nearly linear relationship between them and the correlation coefficient R^2 of linear fitting is 0.98458. The sensitivity of the MRR equals to the slope of the curve, which is about 1.99 GHz/°C.

To demonstrate the frequency tunability of our system, we change the frequency spacing between the carrier and the resonance of the MRR by adjusting the carrier wavelength. It can be seen from Fig. 6(a) that an 8–38 GHz bandpass MPF is obtained. However, limited by the bandwidth of the EA in the OEO, the OEO can only be tuned from 14.60 to 25.65 GHz, as shown in Fig. 6(b). It should be noted that certain frequencies cannot be achieved because of the non-flat frequency response of the devices in the OEO loop.

The stability of the proposed OEO is also verified. Fig. 7 shows the frequency drifting within 25 min. The frequency of the signal drifted by 360 kHz within 25 min, which is due to the lack of stabilization mechanism of the MRR. Since the temperature controller is unavailable in our lab, the effective refractive index of the MRR changes as the drift of the temperatures, leading to the overall drift of the output spectrum of the MRR. The stability of the OEO can be significantly improved by photonic packaging and temperature control.

Table 1 shows the performance comparison with the previous integrated OEO in terms of integration platform, integration degree, SMSR, frequency tunable range, and phase noise. It can be seen that, by utilizing the high-Q MRR presented in this letter, the phase noise is largely improved. However, the integration degree of the proposed OEO is not high enough, which needs to be further improved in future works.

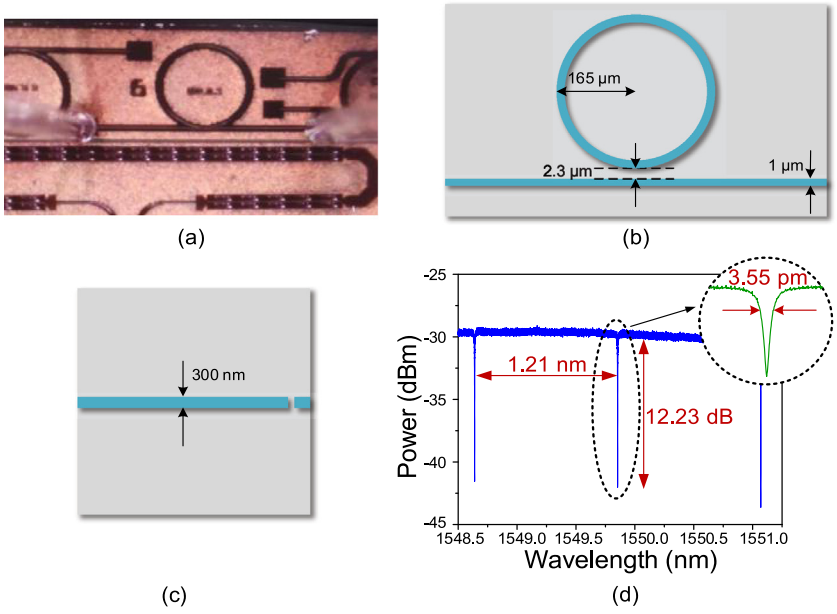

Fig. 2. The proposed MRR. (a) microscope image, (b) vertical view, (c) left view, and (d) spectral response of the MRR.

Table 1
Performance comparison of different OEOs.

Ref.	Integration platform	Integration degree	SMSR/dB	Frequency tunable range/GHz	Phase noise/ dBc/Hz@10 kHz
[5]	SOI	a PM and an MRR	~53@5.9 GHz	5.9–18.2	~−50@5.9 GHz
[8]	SOI	an MRR	52@12.2 GHz	0–20	−95@12.2 GHz
[9]	SOI	a PM, an MDR and a PD	67@4.74 GHz	3.0–7.4	−80@4.74 GHz
[10]	silicon nitride	an MDR	31.1@19.2 GHz	4.0–20.0	−120@19.2 GHz
[11]	InP	the whole OEO system	/	7.30 ± 0.01 8.87 ± 0.01	~−65@7.30 GHz ~−60@8.87 GHz
The paper	silicon nitride	an MRR	49.47@25.65 GHz	14.60–25.65	−88@25.65 GHz

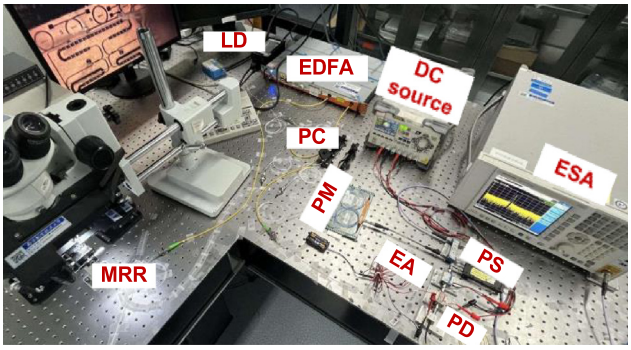

Fig. 3. Picture of the MRR-based OEO. ESA: electrical spectrum analyzer.

4. Conclusion

In conclusion, a tunable OEO by employing a high-Q silicon nitride MRR has been proposed and demonstrated. The FWHM of the MRR is 3.55 pm, so the Q-factor is calculated as 4.36×10^5. By adding it to a phase-modulated link, an 8–38 GHz MPF is achieved and its 3-dB bandwidth is ~610 MHz. Based on the tunable MPF, an OEO that can be tuned within 14.60–25.65 GHz is successfully obtained. The SMSR of the 25.65-GHz oscillation signal reaches 49.47 dB, and the phase noise is −88 dBc/Hz@10 kHz. Further work will focus on improving the integration degree and reducing the phase noise further.

Declaration of competing interest

The authors declare that they have no known competing financial interests or personal relationships that could have appeared to influence the work reported in this paper.

Data availability

Data will be made available on request.

Acknowledgments

This work was supported by the National Key R&D Program of China (2020YFB1805704), the National Natural Science Foundation of China under Grants 62001218, the National Natural Science Foundation of Jiangsu Province, China under Grant BK20200436, the 2021 Jiangsu Shuangchuang Talent Program, China (JSSCBS20210174).

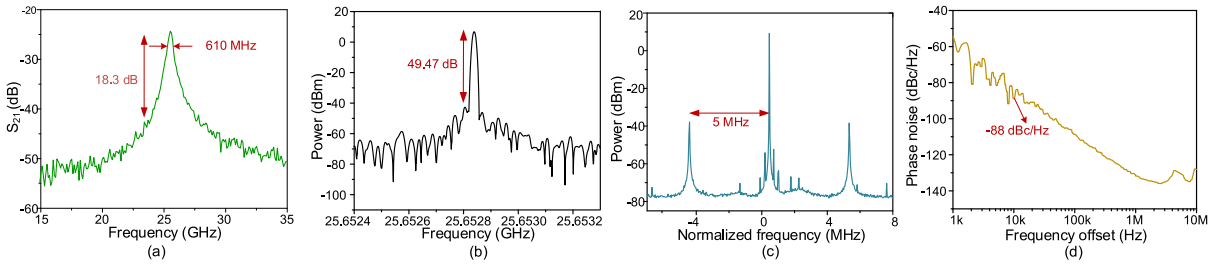

Fig. 4. (a) The frequency response of the bandpass MPF. (b) The electrical spectrum. (c) The FSR of the tunable OEO and (d) phase noise of the 25.65-GHz microwave signal.

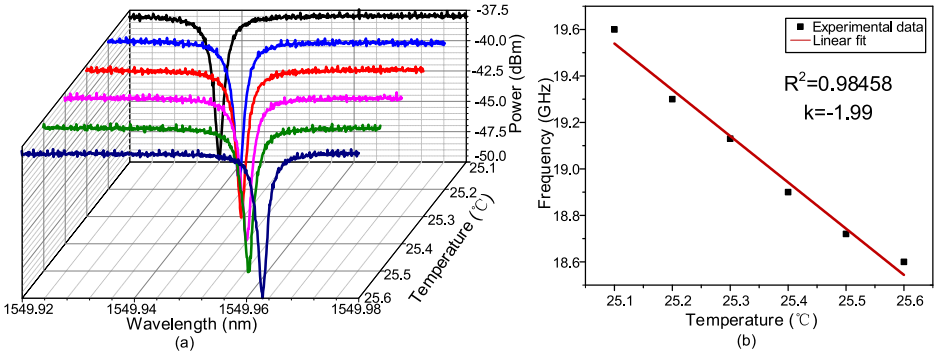

Fig. 5. (a) The temperature variation of the spectral response of the MRR and (b) the corresponding oscillation frequency of the OEO.

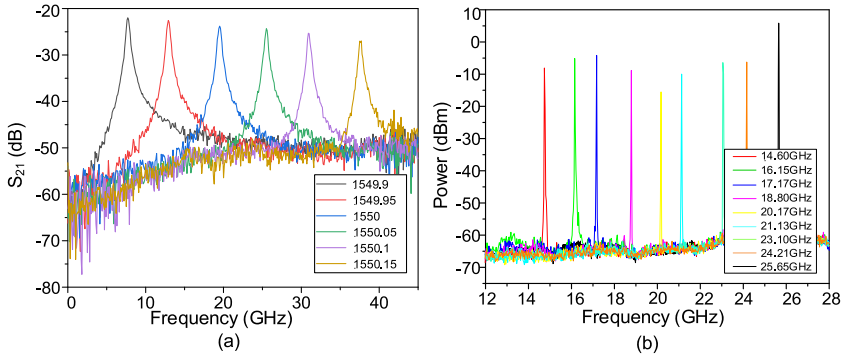

Fig. 6. Tuning range of the (a) MPF and (b) OEO.

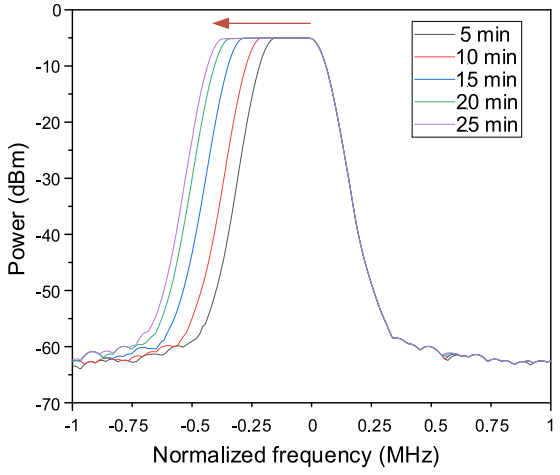

Fig. 7. Stability of the proposed OEO.

References

[1] D. Eliyahu, D. Seidel, L. Maleki, Phase noise of a high performance oeo and an ultra-low noise floor cross-correlation microwave photonic homodyne system, in: 2008 IEEE International Frequency Control Symposium, Honolulu, America, 2008, p. 811.

[2] A. Savchenkov, V. Ilchenko, W. Liang, D. Eliyahu, A. Matsko, L. Maleki, Voltage-controlled photonic oscillator, Opt. Lett. 35 (1572) (2010).

[3] B. Romeira, K. Seunarine, C. Ironside, A. Kelly, J. Figueiredo, A self-synchronized optoelectronic oscillator based on an RTD photodetector and a laser diode, IEEE Photonics Technol. Lett. 23 (1148) (2011).

[4] P. Zhou, S. Pan, D. Zhu, R. Guo, F. Zhang, Y. Zhao, A compact optoelectronic oscillator based on an electroabsorption modulated laser, IEEE Photonics Technol. Lett. 26 (86) (2013).

[5] P. Do, C. Alonso-Ramos, X.Le. Roux, I. Ledoux, B. Journet, E. Cassan, Wideband tunable microwave signal generation in a silicon-micro-ring-based optoelectronic oscillator, Sci. Rep. 10 (1) (2020).

[6] P.T. Do, C. Alonso-Ramos, X. Leroux, D. Pérez-Galacho, L. Vivien, I. Ledoux-Rak, E. Cassan, Silicon photonic micro-ring resonator dedicated to an optoelectronic oscillator loop, in: Silicon Photonics: From Fundamental Research to Manufacturing, Strasbourg, France, 2018, p. 72.

[7] H. Qiu, F. Zhou, J. Qie, Y. Yao, X. Hu, Y. Zhang, X. Xiao, Y. Yu, J. Dong, X. Zhang, A continuously tunable sub-gigahertz microwave photonic bandpass filter based on an ultra-high-Q silicon microring resonator, J. Lightwave Technol. 36 (4312) (2018).

[8] Y. Yu, H. Tang, W. Liu, X. Hu, Y. Zhang, X. Xiao, Y. Yu, X. Zhang, Frequency stabilization of the tunable optoelectronic oscillator based on anultra-high-Q microring resonator, IEEE J. Sel. Top. Quantum Electron. 26 (1) (2019).

[9] W. Zhang, J. Yao, Silicon photonic integrated optoelectronic oscillator for frequency-tunable microwave generation, J. Lightwave Technol. 36 (4655) (2018).

[10] P. Liu, P. Zheng, H. Yang, D. Lin, G. Hu, B. Yun, Y. Cui, Parity-time symmetric frequency-tunable optoelectronic oscillator based on a Si_3N_4 microdisk resonator, Appl. Opt. 60 (1930) (2021).

[11] J. Tang, T. Hao, W. Li, D. Domenech, R. Baños, P. Muñoz, N. Zhu, J. Capmany, M. Li, Integrated optoelectronic oscillator, Opt. Express 26 (12257) (2018).

[12] R. Cong, S. Li, S. Pan, Notch/bandpass microwave photonic filter based on a microring resonator and a LiNbO3 phase modulator, in: 2019 IEEE MTT-S International Wireless Symposium, IWS, Guangzhou, China, 2019, p. 1.

[13] W. Bogaerts, P. De Heyn, T. Van Vaerenbergh, K. De Vos, S. Kumar Selvaraja, T. Claes, P. Dumon, P. Bienstman, D. Van Thourhout, R. Baets, Silicon microring resonators, Laser Photonics Rev. 6 (47) (2012).